

Modelling nanomechanical behaviour of additively manufactured Ti6Al4V alloy

Jelena Srnec Novak^{1,2}, David Liović¹, Ervin Kamenar^{1,2}, Marina Franulović¹

¹University of Rijeka, Faculty of Engineering, Vukovarska 58, 51000 Rijeka, Croatia

²University of Rijeka, Centre for Micro- and Nanosciences and Technologies, Radmile Matejčić 2, 51000 Rijeka, Croatia

jsrrecnovak@riteh.hr

Abstract

This study investigates the elastoplastic behaviour of additively manufactured Ti6Al4V alloy at micro and nano scale using nanoindentation device, imposing different indentation loads. Additionally, finite element analysis (FEA) is employed to obtain numerically load – displacement ($P-h$) curve for varying input parameters. To obtain meaningful results, comparison between experimental and numerical results has been performed to explore the influence of Berkovich tip radius on the load – displacement curve. Finally, it has been observed that FEA enables a reliable estimation of hardness and maximum indentation load at higher loads, exhibiting alignment with experimental curves. When lower indentation loads were used, the differences between numerically and experimentally determined maximum indentation loads were higher. These findings contribute to advancing the understanding of elastoplastic behaviour of additively manufactured Ti6Al4V alloy, when subjected to both high and low indentation loads.

Nanoindentation, elastoplastic material behaviour, numerical analysis, additive manufacturing

1. Introduction

In recent years, additive manufacturing (AM) has become increasingly popular as it offers many benefits over conventional manufacturing methods. As such, understanding the elastoplastic behaviour at the nano and micro scale is crucial, particularly for small and topologically complex components produced with AM techniques. In these components, the reliable determination of the intrinsic mechanical properties is challenging by performing traditional tensile tests. Nevertheless, nanoindentation tests allow determination of material properties (i.e. nano-hardness and Young's modulus) at small-scale and on low-volume specimens that may have complex structures.

It is observed that increasing the strain rate for indentation loads of 10 mN results in a significant reduction in the maximum indentation depth, thereby affecting the elastoplastic behaviour of the Ti6Al4V alloy produced using electron beam powder bed fusion process [1]. However, applying such low loads leads to indentation depths below 300 nm, where higher scatter in Young's modulus and nano-hardness for LB-PBF Ti6Al4V alloy is reported [2]. The elevated data scatter at such low indentation depths is attributed to the highly textured microstructure characteristic of additively manufactured Ti6Al4V alloy [3].

Therefore, in this study, both low and high indentation depths are considered to increase the relevance of the results. In addition, the effectiveness of the employed numerical procedure in estimating elastoplastic response is evaluated by comparison with experimental results on both high and low indentation depths. This paper investigates the possibility of modelling elastoplastic behaviour under indentation load at micro and nanoscale of widely used additively manufactured Ti6Al4V alloy by applying different indentation loads.

2. Materials and methods

Within this research, a total of nine cubic specimens ($10 \times 10 \times 10$ mm³) are produced using the laser beam powder bed fusion (LB-PBF) method with Concept Laser M2 machine. After

manufacturing, all specimens are annealed under argon inert atmosphere by maintaining temperature of 840°C for 2h. Only one specimen is selected to evaluate finite element method (FEM) applicability in modelling of elastoplastic behaviour of Ti6Al4V alloy subjected to different indentation loads. Selected specimen for experimental and numerical investigation is manufactured using laser power of 250 W and scanning speed of 1000 mm/s. Detailed description of LB-PBF process and annealing heat treatment can be found in [2].

To determine nano-hardness, it is necessary to calculate contact stiffness (S), which is defined as slope at the maximum displacement of unload part of $P-h$ curve [4].

$$S = \left. \frac{dP_{\text{unload}}}{dh} \right|_{h=h_{\text{max}}} \quad (1)$$

Furthermore, the projected area of Berkovich tip (A_p) is defined as follows [4]:

$$A_p = 24.56 \cdot h_c^2 + C_1 \cdot h_c \quad (2)$$

where h_c is contact depth, and C_1 is the area coefficient of the Berkovich tip, determined through calibration procedure. Contact depth can be calculated as [4]:

$$h_c = h_{\text{max}} - \varepsilon^* \cdot \frac{P_{\text{max}}}{S} \quad (3)$$

where h_{max} represents maximum displacement, P_{max} maximum load and $\varepsilon^* = 0.75$ is a constant for the Berkovich tip. Nano-hardness (H) is defined as [4]:

$$H = \frac{P_{\text{max}}}{A_p} \quad (4)$$

Equation (5) is used both in experimental and numerical analysis to determine nano-hardness values according to procedure described as follows.

2.1. Nanoindentation experimental procedure

Nanoindentation experiments are performed at room temperature utilizing a three-sided Berkovich diamond indenter mounted on the Nanoindenter Keysight G200. Load controlled mode is used and three different indentation loads (10 mN, 100 mN and 200 mN) are considered to investigate elastoplastic

behaviour both at low and high indentation depths. Prior to nanoindentation experiments, all specimens are grinded, polished and etched using Kroll's reagent.

2.2. Numerical analysis

Numerical simulations are conducted using Abaqus/Standard 2020, with the specimen modelled in 3D, incorporating cyclic symmetry. A 3D model has been chosen to accurately depict the Berkovich tip (three-sided pyramid) and investigate the influence of tip and edges blunting on the results, whereas a 2D model only permits incorporating blunting of the tip without affecting the edges. Utilizing cyclic symmetry enables a reduction in computational time by modelling only one-third of the entire model. This approach resulted in a one-third model, enhancing computational efficiency. The Berkovich tip is treated as a discrete rigid entity with hard and frictionless contact with the specimen. The specimen model (Fig. 1), with a height of 25 μm , and diameter of 20 μm , underwent mesh refinement near the indentation site and gradual coarsening in distant regions to balance computational efficiency and accurate representation of stress and strain gradients. Numerical model of the specimen is defined with a mesh of total 88200 eight-node linear brick elements (C3D8) and 93738 nodes. Young's modulus (E) is determined to be 141 GPa, representing the mean value from Tab. 1 and the Poisson's ratio is set to 0.33 which corresponds to Ti6Al4V alloy [5]. The Johnson-Cook plasticity model is used to model plastic hardening during indentation, with parameters adopted from [6], where $A=997$ MPa, $B=746$ MPa and $n=0.325$. In AM Ti6Al4V alloys, microstructural anisotropy predominantly influences ductility, whereas Young's modulus, yield strength, and tensile strength exhibit negligible directional dependence [7]. Additional analysis assessed the blunting effect of the Berkovich tip radius on the loading section of the $P-h$ curve.

3. Results and discussion

In nanoindentation, indenter blunting is unavoidable. To mitigate this, the standard procedure involves calibration of the Berkovich tip using additional coefficients for the A_p calculation as defined by Equation (3). While this reduces errors in determining E and H , the impact of blunting persists in the elastoplastic response, particularly evident with increased indentation loads, as illustrated in Fig. 1.

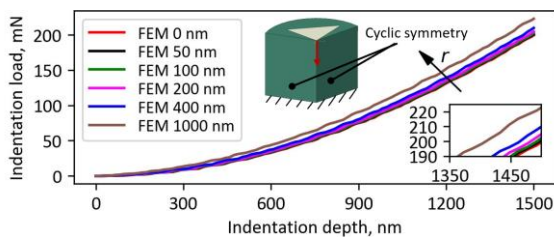


Figure 1. Tip radius influence on loading parts of $P-h$ curves

Increasing the tip radius from 0 to 1000 nm causes an upward shift in the loading regime of the $P-h$ curve, indicating a higher indentation force requirement for the same displacement. The radius of a new and unused Berkovich tip typically ranges from 20 to 100 nm, depending on the manufacturer. Since elastoplastic response for ideally sharp Berkovich tip and Berkovich tip with radius <100 nm is almost identical, the ideally sharp Berkovich tip is used in further analysis. Fig. 2 depicts experimentally and numerically determined $P-h$ curves for three distinct indentation loads. As can be seen, there is a certain discrepancy between experimental and numerical results due to difference in Berkovich tip radius and exact Young's modulus. The Berkovich tip radius in this study may fall outside the usual range of 20 to 100 nm, as trial measurements are performed before the reported measurements in this paper. This preliminary experimental phase might have led to the blunting

of the Berkovich tip, thereby contributing to the observed disparities in the reported results. Furthermore, Young's modulus value of 141 GPa is used for all three simulations, inducing differences particularly in the unloading part of the $P-h$ curve which has elastic nature. Experimentally determined values in Tab. 1 are reported in form of mean value \pm STD. The highest difference between experimentally and numerically determined P_{max} is found when the lowest indentation loads were utilized, while the lowest difference was found when the highest indentation loads are used. Furthermore, hardness values determined both experimentally and numerically are reported in Tab. 1.

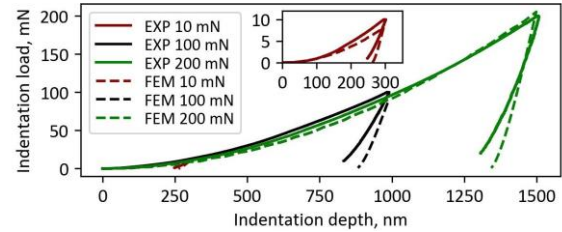


Figure 2. Comparison between experimental and FEM $P-h$ curves

Table 1. Experimentally and numerically determined P_{max} values.

Test ID	E , GPa	$P_{\text{max-exp}}$, mN	$P_{\text{max-sim}}$, mN	Dif., %
10 mN	130 \pm 11	10	8.18	18.2
100 mN	147 \pm 13	100	90.22	9.8
200 mN	146 \pm 19	200	205.39	2.7
Test ID	H_{exp} , GPa	COV, %	H_{sim} , GPa	Dif., %
10 mN	4.417 \pm 0.72	16.3	4.33	2
100 mN	4.654 \pm 0.65	14	4.27	8.3
200 mN	4.038 \pm 0.37	9.2	4.20	4

As can be seen, the differences between H_{exp} and H_{sim} are within the range of variability considering the coefficient of variation (COV). In general, the microstructure of the PBF-LB Ti6Al4V alloy consists of $\alpha+\beta$ laths which have different mechanical properties. Therefore, employing higher indentation loads leads to increased indentation depths, incorporating a greater number of $\alpha+\beta$ laths and thereby reducing their individual effects, resulting in more robust and averaged results.

4. Conclusions and outlook

The application of the FEA methodology in this study enables reliable estimation of nano-hardness and maximum indentation load especially when high indentation depths were used. In that case maximum indentation load and hardness errors were 2.7% and 4%, respectively. However, at lower indentation loads, the presence of higher error in maximum indentation load is notable. Furthermore, the numerically derived $P-h$ curve for the LB-PBF Ti6Al4V alloy under indentation load showed reasonable alignment with the experimentally determined curve further supporting application of proposed FEA approach.

In future work, possibility to obtain stress-strain curves from the experimentally and numerically determined $P-h$ curves for different indentation loads, will be investigated.

Acknowledgements

This study is supported by the Croatian Science Foundation under project number IP-2019-04-3607 and by the University of Rijeka under project numbers uniri-tehnic-18-34 and uniri-mladi-tehnic-22-14. Moreover, the experimental work was made feasible through access to equipment obtained under the ERDF project RC.2.2.06-0001 "RISK."

References

- [1] Peng H et al. 2021 *Materials* **14** 3004
- [2] Liović D et al. 2023 *Materials* **16** 4341
- [3] Cepeda-Jiménez C et al. M 2020 *Mater. Charact.* **163** 110238
- [4] Oliver W C et al. 1992 *J. Mater. Res.* **7** 1564-83
- [5] Xu Y et al. 2019 *J. Mech. Behav. Biomed. Mater.* **99** 225-39
- [6] Wang Z and Li P 2018 *Mater. Sci. Eng. A* **725** 350-58
- [7] Carroll B E et al. 2015 *Acta Mater.* **87** 309-20